ACS Medicinal Chemistry Letters

Featured Letter

Cite This: ACS Med. Chem. Lett. 2020, 11, 16−22

pubs.acs.org/acsmedchemlett

Fluorescence Labeling of Neurotensin(8−13) via Arginine Residues Gives Molecular Tools with High Receptor Affinity

Max Keller,*[,†] Shahani A. Mahuroof,[‡] Vivyanne Hong Yee,[‡] Jessica Carpenter,[‡] Lisa Schindler,[†] Timo Littmann,[†] Andrea Pegoli,[†,§] Harald Hübner,[∥] Günther Bernhardt,[†] Peter Gmeiner,[∥] and Nicholas D. Holliday*[,‡]

[†]Institute of Pharmacy, Faculty of Chemistry and Pharmacy, University of Regensburg, Universitätsstraße 31, D-93053 Regensburg, Germany

[‡]School of Life Sciences, University of Nottingham, Queen's Medical Centre, Nottingham NG7 2UH, United Kingdom

[∥]Department of Chemistry and Pharmacy, Medicinal Chemistry, Friedrich Alexander University, Nikolaus-Fiebiger-Straße 10, D-91058 Erlangen, Germany

Supporting Information

ABSTRACT: Fluorescence-labeled receptor ligands have emerged as valuable molecular tools, being indispensable for studying receptor−ligand interactions by fluorescence-based techniques such as high-content imaging, fluorescence microscopy, and fluorescence polarization. Through application of a new labeling strategy for peptides, a series of fluorescent neurotensin(8−13) derivatives was synthesized by attaching red-emitting fluorophores (indolinium- and pyridinium-type cyanine dyes) to carbamoylated arginine residues in neurotensin(8−13) analogues, yielding fluorescent probes with high NTS_1R affinity (pK_i values: 8.15−9.12) and potency (pEC_{50} values (Ca^{2+} mobilization): 8.23−9.43). Selected fluorescent ligands were investigated by flow cytometry and high-content imaging (saturation binding, kinetic studies, and competition binding) as well as by confocal microscopy using intact CHO-$hNTS_1R$ cells. The study demonstrates the applicability of the fluorescent probes as molecular tools to obtain, for example, information about the localization of receptors in cells and to determine binding affinities of nonlabeled ligands.

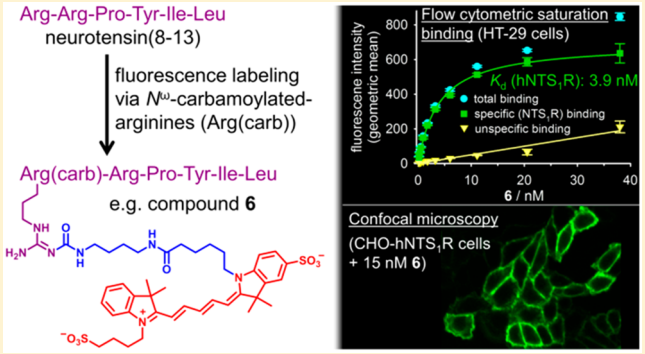

KEYWORDS: *Neurotensin receptor, carbamoylated arginine, fluorescence labeling, flow cytometry, high-content imaging, confocal microscopy*

Neurotensin (NT), a 13 amino acid neuropeptide (cf. Figure 1) which was first isolated and purified from bovine hypothalamus,[1] is mainly found in the gastrointestinal tract and the central nervous system.[2,3] Three transmembrane receptors were identified to mediate the physiological actions of NT: the NTS_1R and NTS_2R, both family A G-protein coupled receptors (GPCRs), and the NTS_3R (sortilin), a member of the Vps10p-domain receptor family.[2,4−6] As the NTS_1R is overexpressed in various malignant tumors such as pancreatic adenocarcinoma, breast cancer, and colorectal carcinoma, it represents a potential target for tumor radiodiagnosis and endoradiotherapy,[7−10] an approach requiring labeled, hydrophilic, stable, and potent NTS_1R ligands. Noteworthily, the carboxy-terminal hexapeptide of NT (NT(8−13), **1**; Figure 1) is equipotent with NT at NTS_1 and NTS_2 receptors.[11]

Generally, the determination of dissociation constants of receptor ligands is fundamental in terms of studying ligand receptor interactions. For this purpose, well characterized labeled receptor ligands, used as tools for competition binding studies, are indispensable. Classical competition binding assays are based on radiolabeled ligands exhibiting high receptor affinity. During the past few decades, fluorescent receptor ligands have gained increasing importance as molecular tools,[12−18] representing an attractive alternative to radioligands, e.g. with respect to safety issues and costs.

Moreover, in contrast to radioligand binding assays, fluorescent ligands enable the measurement of bound ligand under homogeneous conditions both at equilibrium and in kinetic analyses.[22−27]

To date, a few fluorescently labeled NTS_1R ligands have been reported, representing derivatives of NT,[28] NT(2−13),[29] or NT(8−13).[25,30] These fluorescent peptides have in common that the fluorophore was attached to the peptide via the N-terminus, which can result in a considerable decrease in receptor affinity.[30] Recently, a new labeling strategy for arginine-containing peptides, based on the bioisosteric replacement of

Received: October 6, 2019
Accepted: November 19, 2019
Published: November 19, 2019

DOI: 10.1021/acsmedchemlett.9b00462
ACS Med. Chem. Lett. 2020, 11, 16−22

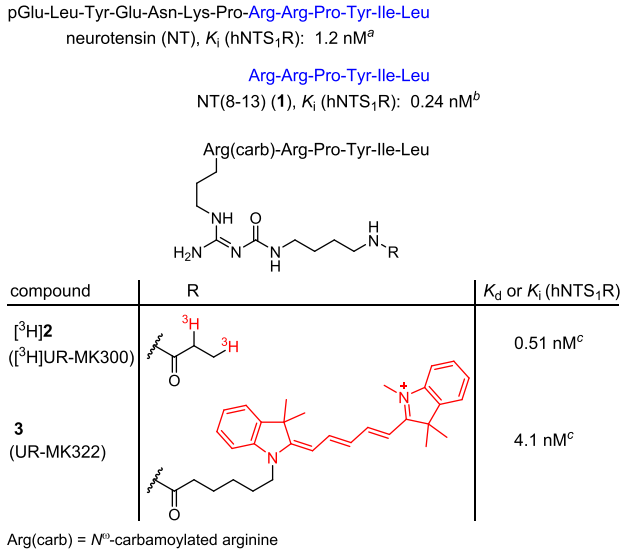

Figure 1. Structures of the tridecapeptide neurotensin, NT(8−13) (**1**, blue), the radiolabeled NT(8−13) derivative [^{3}H]**2**,[19] and the fluorescent NT(8−13) derivative **3**.[19] [a]Granier et al.[20] [b]Einsiedel et al.[21] [c]Keller et al.[19]

arginine by an amino-functionalized, N^{ω}-carbamoylated arginine, was introduced.[19] This proof-of-concept study included derivatives of **1**, for example the radioligand [^{3}H]**2** and the cyanine dye-conjugated peptide **3** (Figure 1). In the previous study, fluorescent ligand **3** was characterized in terms of NTS$_1$R affinity by competition binding with [^{3}H]**2**,[19] but its suitability as molecular tool for fluorescence-based techniques was not explored.

In this study, we conjugated two types of red-emitting fluorophore core structures (indolinium- and pyridinium-type cyanine dyes) to analogues of **1** containing an N^{ω}-carbamoylated arginine in position 8 or 9. The used dyes (indolinium, pyridinium) are excitable with a red (635 nm) and a 488 nm argon laser, respectively, being standard equipment in many instruments. As the physicochemical properties of fluorescent dyes are a crucial factor effecting, e.g. solubility and unspecific interactions of the respective fluorescent ligands in biological systems,[31] we applied three differently substituted indolinium-type dyes (**5**, **8**, **10**; cf. Scheme 1 and Figure 2), accounting for a negative net charge, a positive charge, or no net charge of the fluorophore. All fluorescence-labeled peptides were investigated with respect to NTS$_1$R affinity in radioligand competition binding assays. Selected fluorescent probes (including the previously reported compound **3**[19]) were characterized by flow cytometry, high-content imaging, and confocal microscopy.

The indolinium-type cyanine dye-labeled NT(8−13) derivatives **6**, **9**, **11**, **12**, **16**, and **17** were prepared by treatment of the amino-functionalized precursor peptides **4**, **7**, or **15**,[19] containing an N^{ω}-carbamoylated arginine either in position 8 (**4**, **7**) or in position 9 (**15**) with the succinimidyl esters of the respective dyes (**5**, **8**, or **10**) (Scheme 1). The pyridinium dye-labeled peptide **14** was obtained by treatment of **7** with the pyrylium derivative **13**[32] in the presence of triethylamine (Scheme 1). The reference compounds **19** and **20** (fluorescent "dummy ligands") were prepared from propylamine (**18**) and succinimidyl esters **10** and **5**, respectively (Scheme 1).

The stability of the fluorescently labeled NT(8−13) derivatives **6**, **11**, **14**, and **17** was investigated by incubating

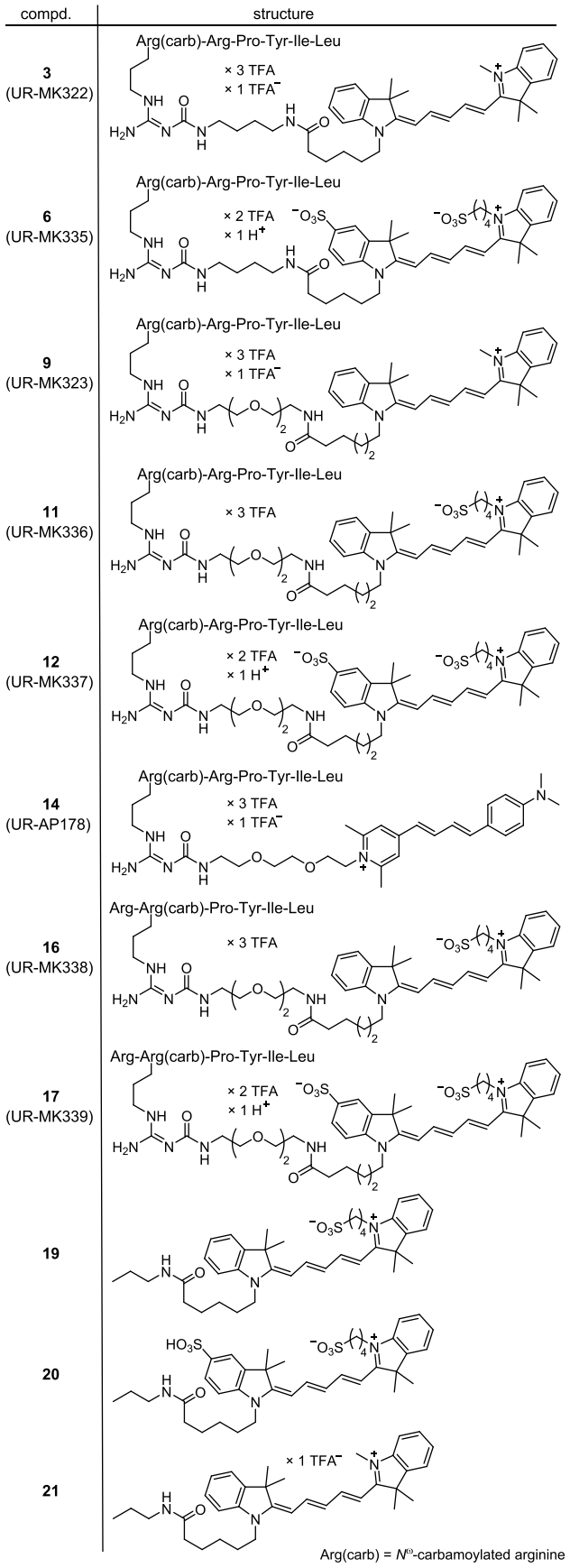

Figure 2. Structures of the synthesized and investigated fluorescent NT(8−13) derivatives **3**,[19] **6**, **9**, **11**, **12**, **14**, **16**, and **17** as well as structures of the fluorescent "dummy ligands" **19**, **20**, and **21**.[19]

DOI: 10.1021/acsmedchemlett.9b00462
ACS Med. Chem. Lett. 2020, 11, 16−22

Scheme 1. Synthesis of the Fluorescent NT(8−13) Derivatives 6, 9, 11, 12, 14, 16, and 17 as well as the Fluorescent "Dummy Ligands" 19 and 20[a]

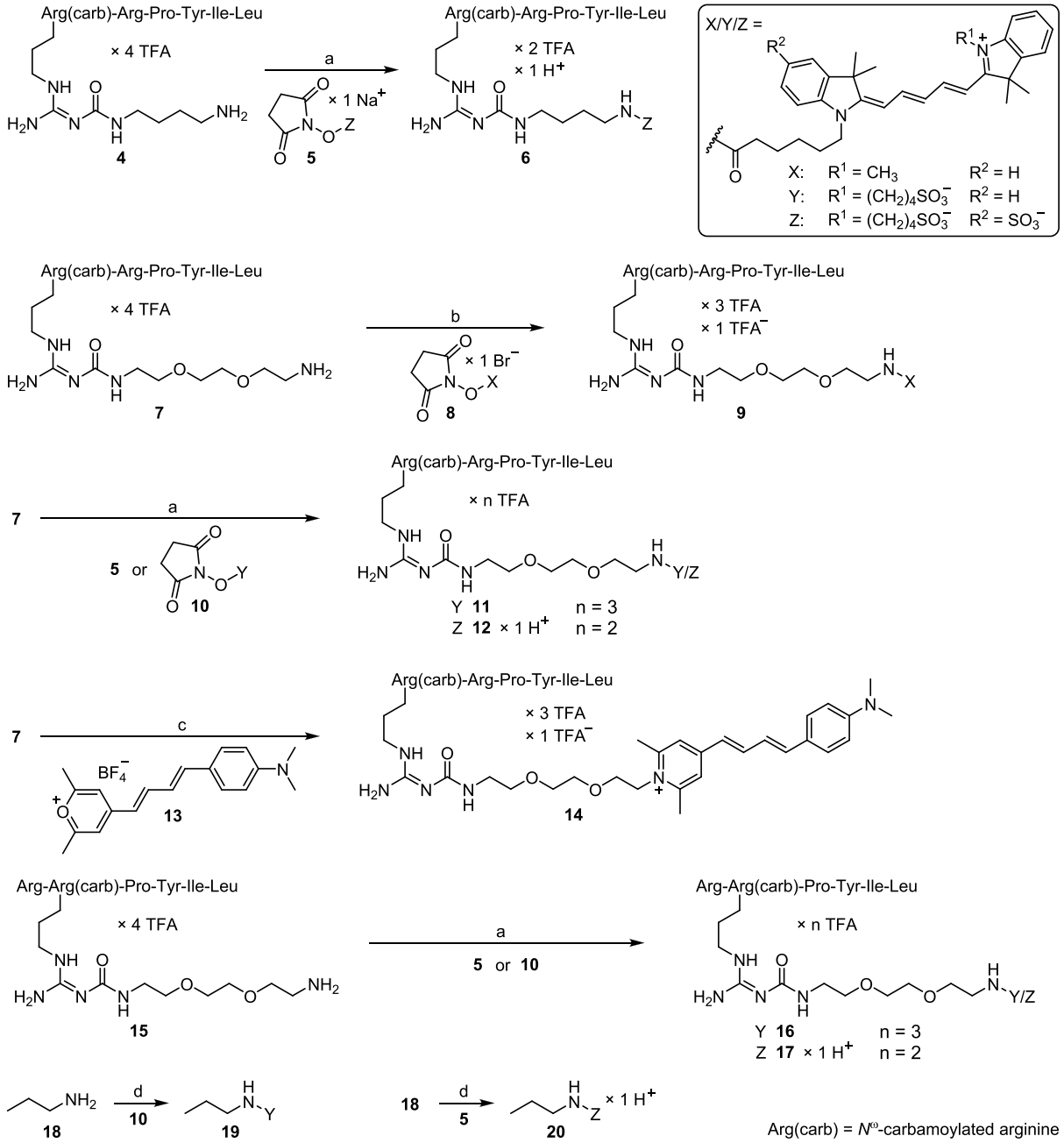

[a]Reagents and conditions: (a) DIPEA, DMF, NMP, rt, 30 min, 42% (**6**), 27% (**11**), 38% (**12**), 24% (**16**), 42% (**17**); (b) DIPEA, $KHCO_3$, DMF, H_2O, rt, 30 min, 26%; (c) triethylamine, DMF, NMP, rt, 2 h, 25%; (d) DIPEA, DMF, rt, 15 min, 27% (**19**), 64% (**20**).

these peptides in PBS, pH 7.4, at 22 °C for up to 48 h followed by RP-HPLC analysis. Whereas indolinium-type cyanine dye-labeled fluorescent probes (**6**, **11**, **17**) exhibited excellent stabilities (Figures S1, S2, and S4, Supporting Information), fluorescent probe **14**, containing a pyridinium-type dye, showed minor decomposition after incubation times >24 h (Figure S3, Supporting Information).

Fluorescence quantum yields were estimated (reference: cresyl violet perchlorate) for the indolinium-type fluorescent probes **3**,[19] **6**, and **11** as well as for the pyridinium-type fluorescent peptide **14** in PBS, pH 7.4, and in PBS supplemented with 1% BSA (Table S1, Figures S5−S8, Supporting Information). For all investigated compounds, fluorescence quantum yields, determined in PBS supplemented with 1% BSA, were higher compared to the quantum yields determined in neat PBS (Table S1, Supporting Information).

NTS_1R binding data of the fluorescent peptides **6**, **9**, **11**, **12**, **14**, **16**, and **17** were determined by competition binding with the NT(8−13) derivative [^{3}H]**2**[19] (for structure, see Figure 1) at intact HT-29 colon carcinoma cells endogenously expressing the $hNTS_1R$[33] but no NTS_2R.[19] In addition, NTS_1R binding data of **3**, **6**, **9**, **11**, **12**, and **14** were determined by competition binding with [^{3}H]**2** at whole Chinese hamster ovary cells stably transfected with the $hNTS_1R$ (CHO-$hNTS_1R$ cells[21]).

DOI: 10.1021/acsmedchemlett.9b00462
ACS Med. Chem. Lett. 2020, 11, 16−22

Table 1. NTS_1R Binding Data (pK_i) of 1, 3, 6, 9, 11, 12, 14, 16, and 17, NTS_2R Binding Data (pK_i) of 1, 3, 6, 9, 12, and 17, pK_d Values of 3, 6, 9, and 12 Determined by Saturation Binding ($hNTS_1R$), and $hNTS_1R$ Potencies (pEC_{50}) of 1, 3, 6, and 12 from Ca^{2+} Assays

	$hNTS_1R$							$hNTS_2R$
compound	pK_i[a]	pK_i[b]	pK_d flow cytometry[c]	pK_d high-content imaging[d]		pEC_{50}		pK_i[g]
				60 min/no wash	75 min/with wash	**1**[e]	**2**[f]	
1	9.89 ± 0.01[h]	n.d.	n.a.	n.a.	n.a.	8.92 ± 0.12	10.16 ± 0.14	9.13 ± 0.07
3	8.38 ± 0.02[h]	8.15 ± 0.03	8.44 ± 0.01	7.82 ± 0.16	8.09 ± 0.04	8.99 ± 0.07	n.d.	8.92 ± 0.15
6	8.86 ± 0.05	8.88 ± 0.12	8.41 ± 0.1	8.20 ± 0.07	8.42 ± 0.21	8.23 ± 0.07	9.38 ± 0.22	8.40 ± 0.05
9	8.66 ± 0.01	8.61 ± 0.08	n.d.	7.99 ± 0.14	8.61 ± 0.29	n.d.	n.d.	9.02 ± 0.06
11	8.37 ± 0.07	8.60 ± 0.05	n.d.	n.d.	n.d.	n.d.	n.d.	n.d.
12	8.70 ± 0.05	8.81 ± 0.03	n.d.	7.59 ± 0.10	8.17 ± 0.22	n.d.	9.43 ± 0.23	8.46 ± 0.14
14	9.12 ± 0.03	8.89 ± 0.09	n.d.	n.d.	n.d.	n.d.	n.d.	n.d.
16	8.57 ± 0.002	n.d.	n.d.	n.d.	n.d.	n.d.	n.d.	8.14 ± 0.02
17	8.45 ± 0.02	n.d.	n.d.	n.d.	n.d.	n.d.	n.d.	n.d.

[a]Determined by radioligand competition binding with [^{3}H]**2** at HT-29 colon carcinoma cells (K_d ([^{3}H]**2**) = 0.55 nM); mean values ± SEM from two (**16**), three (**3**, **6**, **9**, **11**, **12**, **17**), or four (**14**) independent experiments (performed in triplicate). [b]Determined by radioligand competition binding with [^{3}H]**2** at CHO-$hNTS_1R$ cells (K_d ([^{3}H]**2**) = 0.29 nM); mean values ± SEM from three independent experiments (performed in triplicate). [c]Determined by flow cytometric saturation binding at CHO-$hNTS_1R$ cells using PBS as binding buffer; mean values ± SEM from two (**3**) or four (**6**) independent experiments (performed in duplicate). [d]Determined by high-content imaging saturation binding at CHO-$hNTS_1R$ cells (binding buffer: Leibovitz's L15 medium, incubation period: 60 or 75 min); "no wash" indicates that no washing step was performed before the measurement, "with wash" indicates that one washing step was performed shortly before the measurement; mean values ± SEM from four (**3**, **6**, **9**) or five (**12**) (60 min incubation), and three (**9**), four (**3**) or five (**6**, **12**) (75 min incubation) independent experiments (performed in triplicate). [e]Determined in a Fura-2 Ca^{2+} assay at human HT-29 cells; mean values ± SEM from two (**1**) or three (**3**, **6**) independent experiments (performed in singlet). [f]Determined in a Fluo-4 Ca^{2+} assay at CHO-$hNTS_1R$ cells; mean values ± SEM from eight independent experiments (performed in triplicate). [g]Determined by competition binding with [^{3}H]**2** at HEK-$hNTS_2R$ cell homogenates (K_d ([^{3}H]**2**) = 0.79 nM); mean values ± SEM from three (**3**, **6**, **9**), four (**16**), five (**12**), or seven (**1**) independent experiments (performed in triplicate). [h]Data were previously reported as K_i value by Keller et al. and were reanalyzed to give the pK_i value.[19] n.d.: not determined; n.a.: not applicable

The pK_i values of **3**, **6**, **9**, **11**, **12**, and **14**, obtained from these competition binding assays, were in excellent agreement with the pK_i values determined at HT-29 cells (Table 1).

As reported for **3**,[19] the fluorescent NT(8−13) derivatives **6**, **9**, **11**, **12**, **14**, **16**, and **17** exhibited high NTS_1R affinities with pK_i values of 8.15−9.12 (Table 1; competition binding curves shown in Figure S9, Supporting Information). This demonstrated that the recently introduced concept of peptide labeling via the nonclassical bioisosteric replacement of arginine by a functionalized N^{ω}-carbamoylated arginine can be successfully applied to either arginine in **1** (Arg^8: **3**, **6**, **9**, **11**, **12** and **14**, Arg^9: **16** and **17**; cf. Figure 2), even if bulky moieties such as fluorescent dyes are attached. Moreover, these results showed that the type of fluorophore (different core structures and charges; cf. Figure 2) had little impact on receptor binding of the fluorescent peptides. In addition to $hNTS_1R$ affinities, $hNTS_2R$ binding data were determined for peptides **1**, **3**, **6**, **9**, **12** and **16** by competition binding at homogenates of HEK-293 cells, transiently transfected with the $hNTS_2R$, using [^{3}H]**2** as radiolabeled probe (K_d ($hNTS_2R$): 0.79 nM). Whereas $hNTS_2R$ affinities of **3** and **9** proved to be slightly higher compared to their NTS_1R affinities, $hNTS_2R$ binding of **6**, **12** and **16** was marginally lower than $hNTS_1R$ binding (Table 1; competition binding curves shown in Figure S10, Supporting Information). This revealed that N^{ω}-carbamoylation and fluorescence labeling at Arg^8 or Arg^9 of the weakly NTS_1R-selective parent compound **1** did not induce selectivity for either NT receptor subtype, being consistent with the bioisosteric character of the carbamoylated arginine.

Agonist activities at the NTS_1 receptor were studied for compounds **1**, **3**, **6**, and **12** in a Fura-2 (**1**, **3**, **6**) or in a Fluo-4 (**1**, **6**, **12**) Ca^{2+} assay using HT-29 cells and CHO-$hNTS_1R$ cells, respectively (Figure S12A and S12C, Supporting Information; pEC_{50} values shown in Table 1; representative time courses of Fluo-4 fluorescence shown in Figure S13, Supporting Information). The pEC_{50} values of compounds **3**, **6**, and **12**, exhibiting maximal effects (efficacies) comparable to that of **1** (cf. upper curve plateaus in Figure S12A and S12C, Supporting Information) were in good agreement with the respective pK_i values obtained from competition binding experiments with [^{3}H]**2** (Table 1). It should be mentioned that CHO-$hNTS_1R$ cells, used for the Fluo-4 assay, show a considerably higher NTS_1R expression compared to HT-29 cells,[19] used for the Fura-2 assay, presumably resulting in higher Fluo-4 assay potencies compared to Fura-2 assay potencies due to a receptor reserve in CHO-$hNTS_1R$ cells (see pEC_{50} values of compounds **1** and **6**, Table 1). The use of **6** and **12** for studying NTS_1R antagonism of the NTS_1R antagonists SR142948A (**22**) and SR48692 (**23**) (structures see Figure S11, Supporting Information) is described in the Supporting Information.

The fluorescent NT(8−13) derivatives **3** and **6** were studied by flow cytometric saturation binding at CHO-$hNTS_1R$ (**3**, **6**) and HT-29 cells (**6**) (for representative isotherms, see Figure S14, Supporting Information). The obtained pK_d values of **3** and **6** were in excellent agreement with the respective pK_i values from competition binding studies with [^{3}H]**2** (Table 1). Moreover, high-content imaging saturation binding studies were performed with **3**, **6**, **9**, and **12** at CHO-$hNTS_1R$ cells (pK_d values see Table 1, for saturation binding curves, see Figure S15, Supporting Information). A more detailed description of saturation binding studies as well as flow cytometric and high-content imaging competition binding studies (**6**, **12**) and flow cytometric kinetic investigations (**3**, **6**) (NTS_1R) are provided in the Supporting Information.

In addition to flow cytometric and high-content imaging binding studies, binding of **3** (indolinium-type fluorophore with positive net charge), **6** (indolinium-type fluorophore with

DOI: 10.1021/acsmedchemlett.9b00462
ACS Med. Chem. Lett. 2020, 11, 16−22

negative net charge), **11** (indolinium-type fluorophore without net charge), and **14** (pyridinium-type fluorophore with positive net charge) to CHO-hNTS$_1$R cells was investigated by confocal microscopy at 22−25 °C. For all fluorescent probes (**3**, **6**, **11**, **14**), fluorescence appeared to be mainly plasma membrane-associated until approximately 10 min of incubation, followed by a continuous increase in intracellular fluorescence, appearing to be located in vesicles (Figure 3 (**3**, **6**, **11**, **14**) and Movies 1, 3,

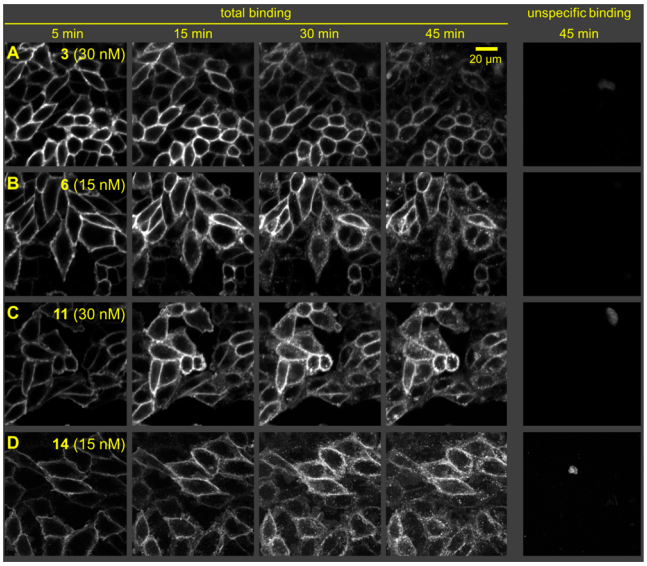

Figure 3. Binding of the cyanine dye labeled fluorescent peptides **3** (fluorophore with positive net charge) (panel A), **6** (fluorophore with negative net charge) (panel B), and **11** (fluorophore with no net charge) (panel C) as well as the pyridinium dye labeled ligand **14** (fluorophore with positive net charge) (panel D) to live CHO-hNTS$_1$R cells at 22−25 °C at the given concentrations, investigated by confocal microscopy (**3**, **6**, and **11**: excitation 633 nm, emission LP 650, **14**: excitation 488 nm, emission LP 560). Images (representative of at least two experiments) were acquired with a LSM 510 confocal microscope after incubation times of 5, 15, 30, and 45 min. Unspecific binding was determined in the presence of **1** (100-fold excess to the fluorescent peptide).

and 7 (**3**, **6**, **11**)). Unspecific binding of **3**, **6**, **11**, and **14** was very low (Figure 3). The observed internalization of NTS$_1$ receptors bound to **3**, **6**, **11**, or **14** was consistent with previous reports on the internalization of NTS$_1$ receptors upon agonist binding.[6,25,30,34] As a representative example, internalization of ligand **6** was also investigated at physiological temperature (37 °C), including a nuclear counterstain (Hoechst dye 33342). These experiments also revealed a fast cellular and vesicular uptake of fluorescent ligand (Figure S21, Supporting Information), which was more pronounced compared to the studies at lower temperature (Figure 3). The dissociation kinetics of **3**, **6**, and **11** studied by confocal microscopy at CHO-hNTS$_1$R cells, revealing recycling of NTS$_1$Rs to the plasma membrane, are described in the Supporting Information.

Interestingly, incubation of CHO-hNTS$_1$R cells with the fluorescent dummy ligands **19** (indolinium-type fluorophore without net charge), **20** (indolinium-type fluorophore with negative net charge), and **21** (indolinium-type fluorophore with positive net charge) revealed a strong cellular uptake of the positively charged compound **21** at a low concentration of 30 nM but no uptake of the neutral and negatively charged compounds **19** and **20**, respectively, applied at a concentration of 200 nM (Figure S22, Supporting Information). This demonstrated that the physicochemical properties of fluorescent dyes should be taken into consideration for the design of fluorescence-labeled biologically active compounds.

In conclusion, we demonstrate that fluorescence labeling of NT(8−13) via carbamoylated arginine residues represents a useful alternative to N-terminal conjugation of fluorescent dyes to NT peptide analogues. The presented fluorescent NTS$_1$R ligands represent useful molecular tools to study NTS$_1$R expression and internalization in cells and determine NTS$_1$R binding affinities of nonlabeled compounds by competition binding, which is useful e.g. for the screening of potential NTS$_1$R ligands and compound profiling in drug development programs. As the fluorescent probes also exhibit high NTS$_2$R affinity, they represent potential molecular tools for fluorescence-based ligand binding studies at the NTS$_2$R. However, due to the missing selectivity, studies of cellular systems or tissues expressing both NT receptor subtypes would be challenging as they require highly selective NTS$_1$R or NTS$_2$R ligands for selective receptor subtype blocking. Regarding unspecific interactions (e.g., adsorption to plastic), fluorescent probes containing a fluorophore with a negative net charge or without net charge proved to be superior to compounds containing a positively charged fluorophore. In conjunction with a recently reported study on the stabilization of the NT(8−13) backbone against enzymatic degradation,[35] the present study can potentially be exploited for the design and preparation of fluorescent and radiolabeled molecular tools useful for the imaging of NTS$_1$R positive tumors.

■ ASSOCIATED CONTENT

Supporting Information

The Supporting Information is available free of charge at https://pubs.acs.org/doi/10.1021/acsmedchemlett.9b00462.

Figures S1−S10; investigation of NTS$_1$R antagonism of SR142948A and SR48692 by the use of fluorescent ligands **6** and **12** (including Figures S11−S13); Tables S1−S3; saturation binding studies with **3**, **6**, **11**, and **12** and competition binding studies with **6** and **12** (including Figures S14−S18); association and dissociation kinetics of **3** and **6** at CHO-hNTS$_1$R cells studied by flow cytometry (including Figures S19 and S20); Figures S21 and S22; association and dissociation kinetics of **3**, **6** and **11** at CHO-hNTS$_1$R cells studied by confocal microscopy (including Figures S23−S30); experimental procedures; data processing; RP-HPLC chromatograms of compounds **6**, **9**, **11**, **12**, **14**, **16**, and **17** (PDF)

Molecular formula strings (XLSX)

Movie 1: Compound **3** association; Figure S23 (AVI)

Movie 2: Compound **3** association and dissociation; Figure S24 (AVI)

Movie 3: Compound **6** association; Figure S25 (AVI)

Movie 4: Compound **6** association and dissociation; Figure S26 (AVI)

Movie 5: Compound **6** association and dissociation; Figure S27 (AVI)

Movie 6: Compound **6** dissociation; Figure S28 (AVI)

Movie 7: Compound **11** association; Figure S29 (AVI)

Movie 8: Compound **11** association and dissociation; Figure S30 (AVI)

DOI: 10.1021/acsmedchemlett.9b00462
ACS Med. Chem. Lett. 2020, 11, 16−22

Movie 9: Addition of 3 nM **1** to CHO-hNTS1R cells (AVI)

Movie 10: Vehicle control for addition of 3 nM **1** to CHO-hNTS1R cells (AVI)

AUTHOR INFORMATION

Corresponding Authors

*E-mail: max.keller@ur.de; Tel.: (+49)941 9433329; Fax: (+49)941 9434820 (M.K.).

*E-mail: Nicholas.Holliday@nottingham.ac.uk; Tel.: (+44)115 8230084 (N.D.H.).

ORCID

Max Keller: 0000-0002-8095-8627

Günther Bernhardt: 0000-0001-6491-9874

Peter Gmeiner: 0000-0002-4127-197X

Present Address

§A.P.: Ramboll Environment & Health GmbH, Werinherstraße 79, 81541 Munich, Germany.

Author Contributions

M.K. and A.P. performed the synthesis. M.K., S.A.M., V.H.Y., J.C., L.S., T.L., H.H., N.H., and P.G. performed functional and binding studies. M.K. initiated and planned the project. M.K., N.D.H., and G.B. supervised the research. M.K., N.D.H., and G.B. wrote the manuscript. All authors have given approval to the final version of the manuscript.

Funding

This work was funded by the Research Grants KE 1857/1-1 and 1-2 of the Deutsche Forschungsgemeinschaft (DFG)) and additionally supported by the Graduate Training Program GRK 1910 of the DFG and the International Doctoral Program "Receptor Dynamics" Elite Network of Bavaria.

Notes

The authors declare no competing financial interest.

Biographies

Max Keller is a medicinal chemist by training and received his doctoral degree at the University of Regensburg under the supervision of Prof. Armin Buschauer. Currently, he is an Assistant Professor at the Institute of Pharmacy, Faculty of Chemistry and Pharmacy, University of Regensburg. His work focuses on the development of molecular tools to study ligand receptor interactions by radiochemical and fluorescence-based methods. Max's main research interest is the design, synthesis, and characterization of selective and labeled ligands of G-protein coupled receptors.

Nick Holliday obtained his Ph.D. and performed postdoctoral work at King's College London, prior to establishing his own research group at the University of Nottingham (UK), where he is now Associate Professor of Pharmacology. His work focuses on developing various bioluminescence and fluorescence imaging methodologies to understand the binding and signaling of G protein coupled receptors and other membrane proteins and the molecular properties of their effector complexes.

ACKNOWLEDGMENTS

The authors thank Elvira Schreiber, Maria Beer-Krön, Brigitte Wenzl, Dita Fritsch, and Susanne Bollwein for excellent technical assistance; Armin Buschauer for providing laboratory equipment; Stephen Briddon for useful discussions; and Seema Rajani and the School of Life Sciences imaging (SLIM) team (University of Nottingham) for their excellent technical support.

ABBREVIATIONS

CHO cells, Chinese hamster ovary cells; DIPEA, diisopropylethylamine; GPCR, G-protein coupled receptor; K_d, dissociation constant obtained from a saturation binding experiment; PBS, phosphate buffered saline; pK_d, negative logarithm of the K_d (in M); pK_i, negative logarithm of the dissociation constant K_i (in M) obtained from a competition binding experiment; TFA, trifluoroacetic acid; Vps10p, vacuolar protein sorting 10 protein.

REFERENCES

(1) Carraway, R.; Leeman, S. E. Isolation of a new hypotensive peptide, neurotensin, from bovine hypothalami. *J. Biol. Chem.* **1973**, *248*, 6854−6861.

(2) Vincent, J.; Mazella, J.; Kitabgi, P. Neurotensin and neurotensin receptors. *Trends Pharmacol. Sci.* **1999**, *20*, 302−309.

(3) Myers, R. M.; Shearman, J. W.; Kitching, M. O.; Ramos-Montoya, A.; Neal, D. E.; Ley, S. V. Cancer, chemistry, and the cell: molecules that interact with the neurotensin receptors. *ACS Chem. Biol.* **2009**, *4*, 503−525.

(4) Vincent, J.-P. Neurotensin receptors: binding properties, transduction pathways, and structure. *Cell. Mol. Neurobiol.* **1995**, *15*, 501−512.

(5) Mazella, J.; Zsürger, N.; Navarro, V.; Chabry, J.; Kaghad, M.; Caput, D.; Ferrara, P.; Vita, N.; Gully, D.; Maffrand, J. P.; Vincent, J. P. The 100-kDa neurotensin receptor is gp95/sortilin, a non-G-protein-coupled receptor. *J. Biol. Chem.* **1998**, *273*, 26273−26276.

(6) Mazella, J.; Vincent, J. P. Internalization and recycling properties of neurotensin receptors. *Peptides* **2006**, *27*, 2488−2492.

(7) Maoret, J.-J.; Pospai, D.; Rouyer-Fessard, C.; Couvineau, A.; Laboisse, C.; Voisin, T.; Laburthe, M. Neurotensin receptor and its mRNA are expressed in many human colon cancer cell lines but not in normal colonic epithelium: binding studies and RT-PCR experiments. *Biochem. Biophys. Res. Commun.* **1994**, *203*, 465−471.

(8) Reubi, J. C.; Waser, B.; Friess, H.; Büchler, M.; Laissue, J. Neurotensin receptors: a new marker for human ductal pancreatic adenocarcinoma. *Gut* **1998**, *42*, 546−550.

(9) Souazé, F.; Dupouy, S.; Viardot-Foucault, V.; Bruyneel, E.; Attoub, S.; Gespach, C.; Gompel, A.; Forgez, P. Expression of neurotensin and NT_1 receptor in human breast cancer: a potential role in tumor progression. *Cancer Res.* **2006**, *66*, 6243−6249.

(10) Morgat, C.; Mishra, A. K.; Varshney, R.; Allard, M.; Fernandez, P.; Hindie, E. Targeting neuropeptide receptors for cancer imaging and therapy: perspectives with bombesin, neurotensin, and neuropeptide-Y receptors. *J. Nucl. Med.* **2014**, *55*, 1650−1657.

(11) Carraway, R.; Leeman, S. E. The amino acid sequence of a hypothalamic peptide, neurotensin. *J. Biol. Chem.* **1975**, *250*, 1907−1911.

(12) Middleton, R. J.; Kellam, B. Fluorophore-tagged GPCR ligands. *Curr. Opin. Chem. Biol.* **2005**, *9*, 517−525.

(13) Kuder, K.; Kiec-Kononowicz, K. Fluorescent GPCR ligands as new tools in pharmacology. *Curr. Med. Chem.* **2008**, *15*, 2132−2143.

(14) Kuder, K. J.; Kiec-Kononowicz, K. Fluorescent GPCR ligands as new tools in pharmacology-update, years 2008- early 2014. *Curr. Med. Chem.* **2014**, *21*, 3962−3975.

(15) Ciruela, F.; Jacobson, K. A.; Fernandez-Duenas, V. Portraying G protein-coupled receptors with fluorescent ligands. *ACS Chem. Biol.* **2014**, *9*, 1918−1928.

(16) Sridharan, R.; Zuber, J.; Connelly, S. M.; Mathew, E.; Dumont, M. E. Fluorescent approaches for understanding interactions of ligands with G protein coupled receptors. *Biochim. Biophys. Acta, Biomembr.* **2014**, *1838*, 15−33.

(17) Stoddart, L. A.; Kilpatrick, L. E.; Briddon, S. J.; Hill, S. J. Probing the pharmacology of G protein-coupled receptors with fluorescent ligands. *Neuropharmacology* **2015**, *98*, 48−57.

(18) Rinken, A.; Lavogina, D.; Kopanchuk, S. Assays with detection of fluorescence anisotropy: challenges and possibilities for character-

DOI: 10.1021/acsmedchemlett.9b00462
ACS Med. Chem. Lett. 2020, 11, 16−22

izing ligand binding to GPCRs. *Trends Pharmacol. Sci.* **2018**, *39*, 187−199.
(19) Keller, M.; Kuhn, K. K.; Einsiedel, J.; Hübner, H.; Biselli, S.; Mollereau, C.; Wifling, D.; Svobodova, J.; Bernhardt, G.; Cabrele, C.; Vanderheyden, P. M.; Gmeiner, P.; Buschauer, A. Mimicking of Arginine by functionalized N^{ω}-carbamoylated arginine as a new broadly applicable approach to labeled bioactive peptides: high affinity angiotensin, neuropeptide Y, neuropeptide FF, and neurotensin receptor ligands as examples. *J. Med. Chem.* **2016**, *59*, 1925−1945.
(20) Granier, C.; van Rietschoten, J.; Kitabgi, P.; Poustis, C.; Freychet, P. Synthesis and characterization of neurotensin analogues for structure/activity relationship studies. Acetyl-neurotensin-(8–13) is the shortest analogue with full binding and pharmacological activities. *Eur. J. Biochem.* **1982**, *124*, 117−124.
(21) Einsiedel, J.; Held, C.; Hervet, M.; Plomer, M.; Tschammer, N.; Hübner, H.; Gmeiner, P. Discovery of highly potent and neurotensin receptor 2 selective neurotensin mimetics. *J. Med. Chem.* **2011**, *54*, 2915−2923.
(22) Allen, M.; Reeves, J.; Mellor, G. High throughput fluorescence polarization: a homogeneous alternative to radioligand binding for cell surface receptors. *J. Biomol. Screening* **2000**, *5*, 63−69.
(23) Veiksina, S.; Kopanchuk, S.; Rinken, A. Budded baculoviruses as a tool for a homogeneous fluorescence anisotropy-based assay of ligand binding to G protein-coupled receptors: the case of melanocortin 4 receptors. *Biochim. Biophys. Acta, Biomembr.* **2014**, *1838*, 372−381.
(24) Stoddart, L. A.; White, C. W.; Nguyen, K.; Hill, S. J.; Pfleger, K. D. G. Fluorescence- and bioluminescence-based approaches to study GPCR ligand binding. *Br. J. Pharmacol.* **2016**, *173*, 3028−3037.
(25) Antoine, T.; Ott, D.; Ebell, K.; Hansen, K.; Henry, L.; Becker, F.; Hannus, S. Homogeneous time-resolved G protein-coupled receptor-ligand binding assay based on fluorescence cross-correlation spectroscopy. *Anal. Biochem.* **2016**, *502*, 24−35.
(26) Sykes, D. A.; Moore, H.; Stott, L.; Holliday, N.; Javitch, J. A.; Lane, J. R.; Charlton, S. J. Extrapyramidal side effects of antipsychotics are linked to their association kinetics at dopamine D_2 receptors. *Nat. Commun.* **2017**, *8*, 1−11.
(27) Stoddart, L. A.; Kilpatrick, L. E.; Hill, S. J. NanoBRET approaches to study ligand binding to GPCRs and RTKs. *Trends Pharmacol. Sci.* **2018**, *39*, 136−147.
(28) Faure, M. P.; Gaudreau, P.; Shaw, I.; Cashman, N. R.; Beaudet, A. Synthesis of a biologically active fluorescent probe for labeling neurotensin receptors. *J. Histochem. Cytochem.* **1994**, *42*, 755−763.
(29) Faure, M. P.; Alonso, A.; Nouel, D.; Gaudriault, G.; Dennis, M.; Vincent, J. P.; Beaudet, A. Somatodendritic internalization and perinuclear targeting of neurotensin in the mammalian brain. *J. Neurosci.* **1995**, *15*, 4140−4147.
(30) Maes, V.; Hultsch, C.; Kohl, S.; Bergmann, R.; Hanke, T.; Tourwe, D. Fluorescein-labeled stable neurotensin derivatives. *J. Pept. Sci.* **2006**, *12*, 505−508.
(31) Nienhaus, G. U.; Nienhaus, K. Fluorescence labeling. In *Fluorescence microscopy: from principles to biological applications*, 2nd ed.; Kubitscheck, U., Ed.; Wiley-VCH: Weinheim, Germany, 2017; pp 133−164.
(32) Wetzl, B. K.; Yarmoluk, S. M.; Craig, D. B.; Wolfbeis, O. S. Chameleon labels for staining and quantifying proteins. *Angew. Chem., Int. Ed.* **2004**, *43*, 5400−5402.
(33) Vita, N.; Laurent, P.; Lefort, S.; Chalon, P.; Dumont, X.; Kaghad, M.; Gully, D.; Le Fur, G.; Ferrara, P.; Caput, D. Cloning and expression of a complementary DNA encoding a high affinity human neurotensin receptor. *FEBS Lett.* **1993**, *317*, 139−142.
(34) Vandenbulcke, F.; Nouel, D.; Vincent, J. P.; Mazella, J.; Beaudet, A. Ligand-induced internalization of neurotensin in transfected COS-7 cells: differential intracellular trafficking of ligand and receptor. *J. Cell Sci.* **2000**, *113* (Pt 17), 2963−2975.
(35) Schindler, L.; Bernhardt, G.; Keller, M. Modifications at Arg and Ile give neurotensin(8−13) derivatives with high stability and retained NTS_1 receptor affinity. *ACS Med. Chem. Lett.* **2019**, *10*, 960−965.

DOI: 10.1021/acsmedchemlett.9b00462
ACS Med. Chem. Lett. 2020, 11, 16−22